

Validation of the CAA solver PIANO with lined-wall boundary condition

Alessandro Bassetti,¹ Sébastien Guérin¹ and Stefan Busse²¹ DLR, Institute of Propulsion Technology, Engine Acoustics, Berlin

e-mail: alessandro.bassetti@dlr.de, sebastien.guerin@dlr.de

² Technische Universität Berlin (TU Berlin), Institute of Fluid Mechanics and Engineering Acoustics**Introduction**

The DLR CAA software PIANO can be used to simulate the time evolution of small-perturbation aerodynamic fields, at the presence of a prescribed background flow. The present work deals with the validation of a slip-wall impedance-type boundary condition (BC) in PIANO. As reported in Ref. [1], the new BC implements the extended Helmholtz-resonator (EHR) model proposed by Rienstra [2]. The implementation follows similar steps as in the work of Richter [3]. In the present paper, the implemented model is briefly summarised; a series of 4 validation cases is then reported.

PIANO and the EHR slip wall

The DLR software PIANO, described in Ref. [4], implements a solver for the linearised Euler equations (LEE). In PIANO the LEE are solved in the time domain by using a finite-difference scheme. High-order approaches are used both in the time marching algorithm (high-order Runge–Kutta method; a 4-stage scheme or a low-dissipation-low-dispersion scheme) and in the spatial discretisation (7-point DRP scheme). In the present work a boundary condition (BC) on the LEE field variables is implemented, to realise a impedance-type wall in PIANO. The implemented BC adopts an EHR model [2] to provide a time-domain description of a locally reacting surface. For an EHR model in the time domain, the perturbation acceleration normal to the impedance surface \dot{u}'_n is a function of the local acoustic pressure p' and perturbation-velocity u'_n (component normal to the impedance surface) [3, 1]. It is expressed as follows:

$$\begin{aligned} \dot{u}'_n(t) = & \frac{1}{m_w} [p'(t) - (R_w + \beta_w) u'_n(t)] \\ & - \frac{e^{-\varepsilon_w}}{m_w} [p'(t - T_w) - (R_w - \beta_w) u'_n(t - T_w)] \\ & + e^{-\varepsilon_w} \dot{u}'_n(t - T_w) \end{aligned} \quad (1)$$

Here the parameters m_w and R_w respectively indicate the face-sheet mass reactance and resistance; β_w , ε_w and T_w are the cavity-reactance coefficient, the cavity resistance and the time delay associated with the EHR model. The impedance associated with the model is defined by the function

$$Z(f) = R_w + j2\pi f m_w - j\beta_w \cot\left(\pi f T_w - j\frac{\varepsilon_w}{2}\right) \quad (2)$$

Compare to Eq. (43) in Ref. [2]. The assignment of the normal perturbation acceleration at a given spatial location on the impedance surface, as in Eq. (1), requires the knowledge of the field variables at the time t and at a past time $t - T_w$. The present implementation projects the normal acceleration assignment, Eq. (1), on the residuals of the Runge–Kutta scheme, depending on the local orientation of the surface normal. The momentum balance at the impedance surface is maintained by using a ghost-point approach.¹ The near-boundary stencil for the pressure variable includes a single ghost point, as for the standard PIANO slip-wall boundary.

¹The previously presented implementation, [1], did not use a ghost-point approach for the momentum balance: the pressure was assigned at the surface and a standard PIANO non-symmetric boundary stencil was used to evaluate the spatial derivative. Furthermore, the surface-normal direction was not general.

Validation of numerical results

A **first** validation test is proposed, where PIANO is used to reproduce experimental measurements of the acoustic-pressure transmission loss on a liner-sample test. We simulate the perturbation field in the DLR-Berlin liner-test rig², described in detail in Ref. [5]. The simulations are proposed in 2D, without a background flow. The computational domain reproduces an axial section of the liner-test rig, including the liner-sample region. The simulated liner sample is the test object introduced in Ref. [6]. The liner sample is modelled by a straight EHR boundary whose length equals the liner-sample axial length. The EHR parameters have been set according to the numerical simulation performed by Richter [6], where a similar boundary treatment was used to model the liner sample. A plane-wave time-harmonic acoustic field is input on a side of the duct. It is then let propagate over the liner sample and further in the hard-wall region. Absorbing boundary conditions are applied at the duct extremities, in order to simulate the anechoic terminations of the rig. A number of time-domain simulations have been performed, with a variation of the input-field frequency. The transmission loss has been evaluated as a function of frequency, by comparing the acoustic-pressure amplitude transmitted through the duct and the input amplitude. Numerically evaluated fluctuating-pressure fields are reported in Fig. 1 (left), at the frequencies 1.1, 1.6 and 2.0 kHz. The numerical evaluation of the transmission coefficient (ratio between transmitted and input pressure amplitudes, P_t/P_i) is compared to the corresponding measurement in Fig. 1 (right).

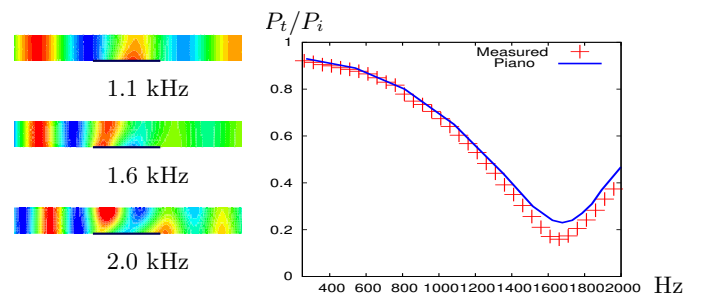


Figure 1: Numerically evaluated acoustic-pressure field in the duct region over the liner sample (black line) in the DLR liner-test facility, test object of Ref. [6], at a given time step (left diagrams). On the right diagram we report a comparison between numerical and experimental estimates for the transmission coefficient.

In a **second** validation test, a plane-wave pressure field is let propagate through a hard-wall S-shaped duct, whose section is equal to the one of the DLR test rig and whose axis is curved. Two separate 3D numerical simulations have been performed in this case: in the first case the duct wall is

²The rig includes a square-section (side 80 mm) rigid-wall duct with an opening, where a liner sample can be fit. The duct has a straight axis and terminates with low-reflection endings. Acoustic excitation is provided by means of loudspeakers, at a frequency below the first high-order-mode cut-on frequency (around 2 kHz). This allows for assuming a plane-wave acoustic-pressure pattern in the hard-wall region of the duct. The liner-sample opening is rectangular and it is at the bottom wall; it is characterised by an axial length of 210 mm and a transverse length of 80 mm. A flow can be introduced in the duct.

modelled by using the standard PIANO slip-wall boundary condition, while in the second case the wall is modelled by using an EHR boundary characterised by very high mass parameter m_W . The coincidence between the solutions at various acoustic-input frequencies demonstrated the correctness of both the projection of the normal-acceleration condition (1) and the corresponding ghost-point pressure correction at varying boundary-normal direction. The result at acoustic-input frequency 3.2 kHz is reported in Fig. 2, where the propagation of the acoustic field occurs from left to right.

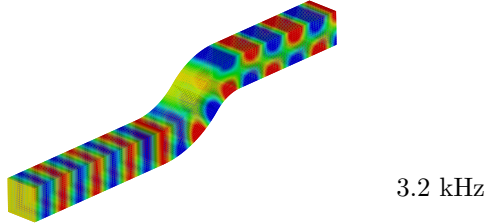


Figure 2: Acoustic-pressure pattern evaluated by modelling the duct boundary with high-mass EHR conditions, i. e. zero normal acceleration is imposed at the wall. Note that the solution is identical to the one obtained by using an analogous slip wall, i. e. zero-normal-velocity boundary condition.

In a **third** test case, the new EHR BC is tested in an application regarding optimal positioning of a lined region in the S-shaped duct of the second validation test. Two identical lined regions have been separately applied. Both regions have EHR characteristics as for the liner-sample surface in the first validation case. They are disposed before, (a), or after, (b), the curved section of the duct (following the propagation direction), see Fig. 3. The simulations have been performed at 4 different frequencies: 0.4, 0.8, 1.6 and 3.2 kHz. While no difference in the transmitted pressure amplitudes has been observed at the 3 lowest frequencies between cases (a) and (b), a larger pressure-amplitude reduction is observed at the highest frequency for case (b), see Fig. 3. This indicates a greater effect of the EHR BC, when subject to an incident acoustic field.

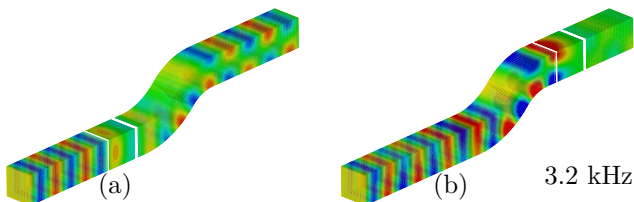


Figure 3: Acoustic-pressure pattern evaluated in the curved-axis duct of Fig. 2 including lined-wall regions. The duct boundaries in the regions between the white lines are modelled by using EHR surfaces (for all the duct-wall sides) with the same parameters as in Fig. 1. The acoustic-input amplitude and frequency are the same as in Fig. 2.

In a **fourth** test case, the pressure scattering due to a segmented (spliced) fan-forward casing liner of an aircraft turbofan engine is simulated. A half-size numerical model has been made for the inlet of a CFM53-6 engine; the inlet has been modelled as a cylindrical duct with diameter equal to half the engine-fan diameter, no background flow has been considered. The acoustic input has been modelled by using the fan-locked (approach condition) modal pressure pattern having azimuthal order equal to the number of blades in the half-scale model: mode (19, 0).³ A simulation with hard-wall condition, Fig. 4 (a), shows the non-propagating

nature of the input acoustic mode, which is cut-off at the given approach-condition blade-passing frequency (BPF). The simulation at the presence of the spliced fan-forward liner, Fig. 4 (b), where the lined surfaces are simulated by using the same EHR model as in the first validation case above, show a complex pressure pattern which propagates through the modelled inlet.

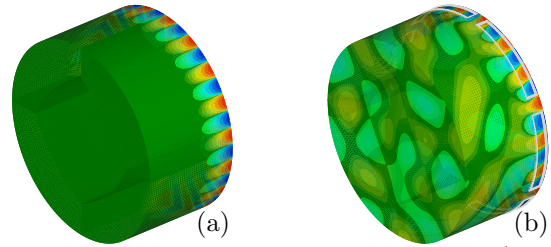


Figure 4: Pressure pattern associated with mode (19,0) of the CFM56-3 fan-section duct. Levels halve with a change of colour. The BC at the inner surface is of uniform slip wall in (a). A spliced casing liner is present for the simulation in (b), where the same EHR boundary condition as in Fig. 1 is used.

Conclusion

The implementation of an extended Helmholtz resonator (EHR) boundary condition (BC) in PIANO has been finalised. A series of validation tests has been conducted, indicating the following:

1. The EHR BC behaves similarly to a corresponding TU-Berlin implementation, Ref. [3].
2. Curved boundaries are correctly handled.
3. The model gives physically sound solutions both in 2D and 3D simulations, in absence of background flow.
4. A high-mass EHR can be used in place of a standard slip-wall BC, with an increase of numerical efficiency.
5. For the used EHR model, an enhanced sound absorption is observed at the presence of incident sound fields.
6. The model can simulate effects such as modal scattering due to liner splices, in realistic aircraft-engine configurations.

Acknowledgements

The present work is part of the project “Bürgernahe Flugzeug am Campus Forschungsflughafen Braunschweig”. The funding, provided by the Bundesland Niedersachsen and by the DLR, is gratefully acknowledged. The simulation of the CFM56-3 liner has been made in cooperation with Deutsche Lufthansa, technical input has been provided by Oliver Bertram, Dirk Schwager, Gerd Saueressig and Helmut Tolksdorf. Lars Enghardt from DLR Berlin contributed to the organisation of this task; he also gave technical input.

References

- [1] Bassetti A, Guérin S and Kornow O; *Introducing lined-wall boundary conditions in the DLR time-domain CAA solver PIANO*, No. 160, p. 211–212, DAGA 2010.
- [2] Rienstra SW; *Impedance models in time domain, including the extended Helmholtz resonator model*, AIAA 2006-2686.
- [3] Richter C; *Liner impedance modelling in the time domain with flow*, PhD Thesis TU Berlin, 2009; ISBN 978-3-7983-2186-1.
- [4] Delfs JW, Bauer M, Ewert R, Grogger HA, Lummer M and Lauke TGW; *Numerical simulation of aerodynamic noise with DLR’s aeroacoustic code PIANO*, Manual of PIANO version 5.2; DLR Braunschweig, January 2008.
- [5] Busse S, Richter C, Thiele F, Heuwinkel C, Enghardt L, Röhle I, Michel U, Ferrante P and Scofano A; *Impedance deduction based on insertion loss measurements of liners under grazing flow conditions*, AIAA 2008-3014.
- [6] Busse S, Richter C, Kückens C, Müller U, Enghardt L and Thiele F; *Experimental and numerical characterisation of a non-locally reacting liner*, p. 1254–1257, NAG/DAGA 2009.

³The number of blades is halved in the half-scale model. While 38 fan blades are present in the CFM53-6 engine, we use in the model the mode with azimuthal order 19 and radial order 0.